

World Journal of *Gastroenterology*

World J Gastroenterol 2019 July 7; 25(25): 3108-3282



**OPINION REVIEW**

- 3108** Advanced imaging in surveillance of Barrett's esophagus: Is the juice worth the squeeze?
Cerrone SA, Trindade AJ
- 3116** Fate plasticity in the intestine: The devil is in the detail
Buczacki S

REVIEW

- 3123** Revisiting the liver's role in transplant alloimmunity
Abrol N, Jadowiec CC, Taner T
- 3136** Hepatocellular carcinoma: Therapeutic advances in signaling, epigenetic and immune targets
Neureiter D, Stintzing S, Kiesslich T, Ocker M
- 3151** Hepatocellular carcinoma: Mechanisms of progression and immunotherapy
Jiang Y, Han QJ, Zhang J

MINIREVIEWS

- 3168** Epidemiology of hepatitis E in South-East Europe in the "One Health" concept
Mrzljak A, Dinjar-Kujundzic P, Jemersic L, Prpic J, Barbic L, Savic V, Stevanovic V, Vilibic-Cavlek T
- 3183** Infections with *Helicobacter pylori* and challenges encountered in Africa
Smith S, Fowora M, Pellicano R

ORIGINAL ARTICLE**Basic Study**

- 3196** Sporamin suppresses growth of xenografted colorectal carcinoma in athymic BALB/c mice by inhibiting liver β -catenin and vascular endothelial growth factor expression
Yang C, Zhang JJ, Zhang XP, Xiao R, Li PG
- 3207** Silicone-covered biodegradable magnesium stent for treating benign esophageal stricture in a rabbit model
Yang K, Cao J, Yuan TW, Zhu YQ, Zhou B, Cheng YS
- 3218** Nuclear magnetic resonance-based metabolomics and metabolic pathway networks from patient-matched esophageal carcinoma, adjacent noncancerous tissues and urine
Liang JH, Lin Y, Ouyang T, Tang W, Huang Y, Ye W, Zhao JY, Wang ZN, Ma CC

Retrospective Study

- 3231** Prevalence and risk factors for Barrett's esophagus in Taiwan
Chen YH, Yu HC, Lin KH, Lin HS, Hsu PI

- 3242** Gut microbiota contributes to the distinction between two traditional Chinese medicine syndromes of ulcerative colitis
Zhang YL, Cai LT, Qi JY, Lin YZ, Dai YC, Jiao N, Chen YL, Zheng L, Wang BB, Zhu LX, Tang ZP, Zhu RX

Observational Study

- 3256** Assessing significant fibrosis using imaging-based elastography in chronic hepatitis B patients: Pilot study
Park HS, Choe WH, Han HS, Yu MH, Kim YJ, Jung SI, Kim JH, Kwon SY

META-ANALYSIS

- 3268** Botulinum toxin injections after surgery for Hirschsprung disease: Systematic review and meta-analysis
Roorda D, Abeln ZA, Oosterlaan J, van Heurn LW, Derikx JP

RETRACTION NOTE

- 3281** Retraction Note: Construction of Gpm6a/ReelinGFP-CreERT2 by BAC recombination using a specific gene in hepatic mesothelial or stellate cells
Shi HB, Lou JL, Shi HL, Ren F, Chen Y, Duan ZP

ABOUT COVER

Editorial board member of *World Journal of Gastroenterology*, Tatsuo Kanda, MD, PhD, Associate Professor, Division of Gastroenterology and Hepatology, Department of Internal Medicine, Nihon University School of Medicine, Tokyo 173-8610, Japan

AIMS AND SCOPE

World Journal of Gastroenterology (*World J Gastroenterol*, *WJG*, print ISSN 1007-9327, online ISSN 2219-2840, DOI: 10.3748) is a peer-reviewed open access journal. The *WJG* Editorial Board consists of 701 experts in gastroenterology and hepatology from 58 countries.

The primary task of *WJG* is to rapidly publish high-quality original articles, reviews, and commentaries in the fields of gastroenterology, hepatology, gastrointestinal endoscopy, gastrointestinal surgery, hepatobiliary surgery, gastrointestinal oncology, gastrointestinal radiation oncology, etc. The *WJG* is dedicated to become an influential and prestigious journal in gastroenterology and hepatology, to promote the development of above disciplines, and to improve the diagnostic and therapeutic skill and expertise of clinicians.

INDEXING/ABSTRACTING

The *WJG* is now indexed in Current Contents®/Clinical Medicine, Science Citation Index Expanded (also known as SciSearch®), Journal Citation Reports®, Index Medicus, MEDLINE, PubMed, PubMed Central, and Scopus. The 2019 edition of Journal Citation Report® cites the 2018 impact factor for *WJG* as 3.411 (5-year impact factor: 3.579), ranking *WJG* as 35th among 84 journals in gastroenterology and hepatology (quartile in category Q2). CiteScore (2018): 3.43.

RESPONSIBLE EDITORS FOR THIS ISSUE

Responsible Electronic Editor: *Yu-Jie Ma*

Proofing Production Department Director: *Yun-Xiaojuan Wu*

NAME OF JOURNAL

World Journal of Gastroenterology

ISSN

ISSN 1007-9327 (print) ISSN 2219-2840 (online)

LAUNCH DATE

October 1, 1995

FREQUENCY

Weekly

EDITORS-IN-CHIEF

Subrata Ghosh, Andrzej S. Tarnawski

EDITORIAL BOARD MEMBERS

<http://www.wjgnet.com/1007-9327/editorialboard.htm>

EDITORIAL OFFICE

Ze-Mao Gong, Director

PUBLICATION DATE

July 7, 2019

COPYRIGHT

© 2019 Baishideng Publishing Group Inc

INSTRUCTIONS TO AUTHORS

<https://www.wjgnet.com/bpg/gerinfo/204>

GUIDELINES FOR ETHICS DOCUMENTS

<https://www.wjgnet.com/bpg/GerInfo/287>

GUIDELINES FOR NON-NATIVE SPEAKERS OF ENGLISH

<https://www.wjgnet.com/bpg/gerinfo/240>

PUBLICATION MISCONDUCT

<https://www.wjgnet.com/bpg/gerinfo/208>

ARTICLE PROCESSING CHARGE

<https://www.wjgnet.com/bpg/gerinfo/242>

STEPS FOR SUBMITTING MANUSCRIPTS

<https://www.wjgnet.com/bpg/GerInfo/239>

ONLINE SUBMISSION

<https://www.f6publishing.com>



Basic Study

Nuclear magnetic resonance-based metabolomics and metabolic pathway networks from patient-matched esophageal carcinoma, adjacent noncancerous tissues and urine

Jia-Hao Liang, Yan Lin, Ting Ouyang, Wan Tang, Yao Huang, Wei Ye, Jia-Yun Zhao, Zhe-Ning Wang, Chang-Chun Ma

ORCID number: Jia-Hao Liang (0000-0002-6288-6288); Yan Lin (0000-0002-8284-9029); Ting Ouyang (0000-0003-4710-3069); Wan Tang (0000-0003-0404-1494); Yao Huang (0000-0001-5616-7828); Wei Ye (0000-0003-1459-0155); Jia-Yun Zhao (0000-0003-2446-2288); Zhe-Ning Wang (0000-0003-3754-0943); Chang-Chun Ma (0000-0002-5389-4250).

Author contributions: Lin Y conceived and designed the experiments; Liang JH and Lin Y contributed to NMR data acquisition; Liang JH, Ouyang T, Tang W and Huang Y analyzed the data; Lin Y wrote the paper; Ye W, Zhao JY and Wang ZN contributed to sample preparation; all authors approved the final version of the manuscript for publication.

Supported by the National Natural Science Foundation of China, No. 81471729 and No. 81101102; the Science and Technology and Planning Project of Guangdong Province, No. 2016A020216025; the Research Award Fund for Outstanding Young Teachers in Higher Education Institutions, Guangdong Province, No. YQ2015245; the National Natural Science Foundation of Guangdong Province, No. S2011010004973; the Department of Education of Guangdong Province, No. 2017KTSCX071.

Institutional review board statement: This study was

Jia-Hao Liang, Yan Lin, Ting Ouyang, Wan Tang, Yao Huang, Wei Ye, Jia-Yun Zhao, Zhe-Ning Wang, Department of Radiology, Second Affiliated Hospital, Shantou University Medical College, Shantou 515041, Guangdong Province, China

Chang-Chun Ma, Department of Radiation Oncology, Affiliated Tumor Hospital, Shantou University Medical College, Shantou 515041, Guangdong Province, China

Corresponding author: Yan Lin, PhD, Chief Doctor, Department of Radiology, Second Affiliated Hospital, Shantou University Medical College, No. 69, Dongshabei Road, Shantou 515041, Guangdong Province, China. 994809889@qq.com
Telephone: +86-13502958156

Abstract

BACKGROUND

Several studies have demonstrated a correlation between esophageal cancer (EC) and perturbed urinary metabolomic profiles, but none has described the correlation between urine metabolite profiles and those of the tumor and adjacent esophageal mucosa in the same patient.

AIM

To investigate how urinary metabolic phenotypes were linked to the changes in the biochemical landscape of esophageal tumors.

METHODS

Nuclear magnetic resonance-based metabolomics were applied to esophageal tumor tissues and adjacent normal mucosal tissues alongside patient-matched urine samples.

RESULTS

Analysis revealed that specific metabolite changes overlapped across both metrics, including glucose, glutamate, citrate, glycine, creatinine and taurine, indicating that the networks for metabolic pathway perturbations in EC, potentially involved in but not limited to disruption of fatty acid metabolism, glucose and glycolytic metabolism, tricarboxylic acid cycle and glutaminolysis. Additionally, changes in most urinary biomarkers correlated with changes in biomarker candidates in EC tissues, implying enhanced energy production for rapid cell proliferation.

reviewed and approved by the Second Affiliated Hospital, Shantou University Medical College Review Board (2018-44).

Informed consent statement:

Informed consent was obtained from each subject prior to participation in this study.

Conflict-of-interest statement:

The authors declare that they have no competing interests related to this study.

Open-Access:

This article is an open-access article which was selected by an in-house editor and fully peer-reviewed by external reviewers. It is distributed in accordance with the Creative Commons Attribution Non Commercial (CC BY-NC 4.0) license, which permits others to distribute, remix, adapt, build upon this work non-commercially, and license their derivative works on different terms, provided the original work is properly cited and the use is non-commercial. See: <http://creativecommons.org/licenses/by-nc/4.0/>

Manuscript source: Unsolicited manuscript

Received: January 25, 2019

Peer-review started: January 25, 2019

First decision: February 26, 2019

Revised: May 13, 2019

Accepted: May 31, 2019

Article in press: June 1, 2019

Published online: July 7, 2019

P-Reviewer: Hashimoto N, Luyer MDP

S-Editor: Cui LJ

L-Editor: Filipodia

E-Editor: Ma YJ



CONCLUSION

Overall, these associations provide evidence for distinct metabolic signatures and pathway disturbances between the tumor tissues and urine of EC patients, and changes in urinary metabolic signature could reflect reprogramming of the aforementioned metabolic pathways in EC tissues. Further investigation is needed to validate these initial findings using larger samples and to establish the underlying mechanism of EC progression.

Key words: Esophageal cancer; Metabolites; Metabolic pathways; Nuclear magnetic resonance-based metabolomics; Tumor tissue; Urine

©The Author(s) 2019. Published by Baishideng Publishing Group Inc. All rights reserved.

Core tip: Our research provides evidence for distinct metabolic signatures and metabolic pathway disturbances between the tumor tissues and urine of esophageal cancer patients, and changes in the urinary metabolic signature could reflect reprogramming of aforementioned metabolic pathways in esophageal tumor tissues.

Citation: Liang JH, Lin Y, Ouyang T, Tang W, Huang Y, Ye W, Zhao JY, Wang ZN, Ma CC. Nuclear magnetic resonance-based metabolomics and metabolic pathway networks from patient-matched esophageal carcinoma, adjacent noncancerous tissues and urine. *World J Gastroenterol* 2019; 25(25): 3218-3230

URL: <https://www.wjgnet.com/1007-9327/full/v25/i25/3218.htm>

DOI: <https://dx.doi.org/10.3748/wjg.v25.i25.3218>

INTRODUCTION

Esophageal cancer (EC) is the eighth most common type of malignant tumor and the sixth leading cause of cancer-related death worldwide^[1]. Identifying cancer-related biomarkers of EC is essential for its diagnosis and therapeutic intervention in the early stage, which in turn will significantly increase patient survival. While there are a few diagnostic/screening techniques, such as upper gastrointestinal endoscopy, endoscopy-based balloon cytology, and serum carcinoembryonic antigen (commonly known as CEA) test, high-throughput and sensitive molecular tools are required to elucidate specific disease biomarkers for optimal disease management. Metabolomics, in which the global changes of small molecular weight metabolites in a given biological specimen are investigated, has considerable potential to identify useful biomarkers, thereby stratifying subjects into disease or nondiseased categories^[2,3]. Proton nuclear magnetic resonance (¹H-NMR) spectroscopy is a well-established, robust, noninvasive and reproducible method for quantifying metabolic profiles^[4], and it has several advantages over other analytical techniques, such as liquid chromatography mass spectroscopy and gas chromatography mass spectroscopy, including nondestructive analysis of samples, minimal sample preparation, and the ability to detect multiple metabolites within a single experiment^[5-8]. NMR data combined with multivariate statistical analysis, such as orthogonal partial least squares discriminant analysis (OPLS-DA), which can be utilized for disease classification (through the use of score plots) and biomarker detection (through the use of loading plots), allow for the identification of potential biomarkers in biological specimens and improve the ability to identify specific metabolic pathways and networks associated with the disease process.

Urine is a biological fluid commonly used by NMR-based metabolomics^[9,10] because it is easily collected in large volumes with noninvasive procedures and may provide substantial diagnostic information for many cancer types^[7,11-13]. Biomarkers in urine may be derived from cell apoptosis, glomerular filtration of blood plasma, cell sloughing, epithelial cell secretion of exosomes, and other processes^[14]. Several NMR spectroscopy-based metabolomic studies have reported that metabolite compositions of urine samples from EC patients differ from those of healthy controls (HCs)^[15,16]. However, little is known about the systemic mechanistic link between esophageal tissues and urine, owing to the invasiveness of tissue sampling and sensitivity of the urinary metabolome to factors such as environment, food and genetic composition.

The aim of this research was to profile parallel metabolites of EC tissues and ad-

adjacent noncancerous tissues alongside urine samples from the same patients, to investigate how urinary metabolomic phenotypes associate with tumor tissue, and to identify specific disturbed metabolic pathways in esophageal tissues and urine. Such information would be vital to bridge the gap between the systemic metabolic characteristics of EC tissues and the corresponding samples of urine and may help advance the utility of urinary-based metabolites as relevant indicators of EC tissue microenvironment.

MATERIALS AND METHODS

Patient recruitment and sample collection

This study was approved by the Ethics Committee of Shantou University Medical College. Written informed consent was obtained from each subject prior to participation. Early-morning midstream urine samples were collected preoperatively from 41 EC patients and 40 HCs between August 2015 and October 2016 at the Second Affiliated Hospital of Shantou University Medical College. EC patients were diagnosed by microscopy, biopsy, or surgical resection, and the disease stage was determined according to the American Joint Committee on Cancer (AJCC) staging system for esophageal tumors: Stage I/II, 15 patients; stage III, 11 patients; stage IV, 15 patients. Each urine sample was mixed with 50 μ L sodium azide preservative and stored at -80°C until further analysis. Patient-matched EC tissues and their corresponding adjacent noncancerous tissues (~ 5 cm away from the tumor margin) were collected from 20 EC patients and immediately stored at -80°C until NMR analysis. Exclusion criteria for all participants included use of antibiotics, nonsteroidal anti-inflammatory drugs, statins, or probiotics within 2 mo of study participation. Additional exclusion criteria for EC patients included chemotherapy or radiotherapy prior to surgery. The demographic and clinical characteristics of the EC patients and controls are summarized in Table 1.

Urine sample preparation

Frozen urine samples were thawed at room temperature and mixed to suspend any settled precipitate. After adding 300 μ L PBS/ D_2O buffer (0.1 M, pH 7.4) to 600 μ L of each urine sample, the mixture was homogenized by vortexing for 60 s and then centrifuged at 8000 rpm for 10 min. Subsequently, a volume of 500 μ L of the supernatant was transferred into an Eppendorf vial, to which 50 μ L of a stock solution of sodium (3-trimethylsilyl)-2, 2, 3, 3-tetradeuteriopropionate (TSP)/ D_2O was added, using a chemical shift reference (0.0 ppm) for spectral alignment. Finally, the resulting mixture was centrifuged at 10000 rpm for 5 min, and 500 μ L of the prepared sample was transferred into a 5-mm high-resolution NMR tube for ^1H -NMR analysis.

Tissue sample preparation

The frozen tissue samples weighed ~ 300 mg and were thawed and cut into small pieces at room temperature. After adding 1.8 mL mixture containing 0.6 mL distilled water (2 mL/g tissue) and 1.2 mL methanol (4 mL/g tissue), the resulting mixture was homogenized at 16000 rpm for 80 s. After homogenization, the mixture was added to chloroform (4 mL/g tissue) and distilled water (4 mL/g tissue) and vortexed for 60 s. The suspension was then left on ice for 15 min and centrifuged at 2000 rpm for 5 min to facilitate separation of the liquid layers. The resulting supernatant was evaporated under a stream of nitrogen and then dried under vacuum for a minimum of 18 h. Subsequently, the lyophilized powder was redissolved with 550 μ L PBS/ D_2O buffer (0.1 mol/L, pH 7.4), to which 50 μ L of a stock solution of TSP/ D_2O was added. After homogenization and centrifugation at 10000 rpm for 5 min, 500 μ L supernatant was transferred into a 5-mm high-resolution NMR tube for ^1H -NMR analysis.

^1H -NMR analysis

All samples were detected by a Bruker AVII 400 MHz NMR spectrometer (Bruker Biospin, Germany) operating at a ^1H frequency of 400.13 MHz. Magnetic field homogeneity was optimized by gradient or manual shimming prior to acquisition. The temperature was maintained at 298 K and lock performed on the D_2O signal. ^1H NMR spectra of urine samples were obtained using a 1D nuclear Overhauser enhancement spectroscopy pulse sequence [RD- 90° -t1- 90° -tm- 90° -ACQ], with the following acquisition parameters: Recycle delay (RD) 1.5 s; t1 3 μ s; mixing time, tm 100 ms; 90° pulse width 7.3 μ s; number of scans (NS) 256; number of points, TD 32768; spectral width (SW) 8012.82 Hz; acquisition time (AQ) 2.04 s. Water suppression was achieved by irradiation of the water peak during RD and tm. Esophageal tissue ^1H NMR spectra were recorded using a standard (1D) Carr-Purcell-Meiboom-Gill pulse sequence with the following acquisition parameters: number of dummy scans 4; RD

Table 1 Summary of clinical and demographic features for study subjects and tumor characteristics

	EC	HC	χ^2	P value
Subjects, <i>n</i>	41	40		
Age (median, range), yr	60, 39-77	59, 28-78		
Sex			6.77	0.12
Male	31	19		
Female	10	21		
Cancer stage				
Stage I/II	15	-		
Stage III	11	-		
Stage IV	15	-		
CEA, ng/mL				
Positive	2	-		
Negative	31	-		
Not measured	8	-		
CA 19-9, U/mL				
Positive	2	-		
Negative	18	-		
Not measured	21	-		
Location				
Cervical	1	-		
Upper thoracic	5	-		
Middle thoracic	24	-		
Lower thoracic	11	-		
Symptoms				
Dysphagia	40	-		
Gastroesophageal reflux	27	-		

EC: Esophageal cancer; HC: Healthy control; CA 19-9: Carbohydrate antigen 19-9; CEA: Carcinoembryonic antigen.

70 ms; 90° pulse width 10 μ s; NS 64; TD 65536; SW 8012 Hz; AQ 4.09 s.

¹H NMR spectral data processing

All free induction decays from 1D ¹H-NMR of the tissues and urine samples were multiplied by a 0.3 Hz exponential line broadening prior to Fourier transformation. ¹H-NMR spectra were then corrected for phase and baseline distortion and calibrated to TSP at 0.0 ppm by using MestReNova software (version 8.1.0, Mestrelab Research, Santiago de Compostella, Spain). To reduce the complexity of the NMR data, the spectral range from 0.8 to 9.0 ppm was segmented into buckets with the equal width of 0.004 ppm. The region of 5.5–4.5 ppm was discarded to eliminate imperfect water suppression. Each bucket was internally normalized to the total integral of the spectrum prior to pattern recognition analysis, to eliminate the dilution or bulk mass differences among samples due to the different sample weight.

Pattern recognition analysis and cross validation

To maximize class discrimination between EC patient and HC urine samples, as well as between EC tissues and their corresponding noncancerous tissues, multivariate data analysis was applied to the ¹H-NMR spectral data according to previously published and accepted methods^[6,7]. The normalized NMR spectral data sets were unit variance scaled and analyzed using the SIMCA-P+ program (version 14.1, Umetrics AB; Umea, Sweden). OPLS-DA was applied to the analysis of ¹H-NMR spectral data to optimize the separation between experimental groups. The model quality was evaluated with the R²Y and Q² values, reflecting the explained fraction of variance and the model predictability. R²Y scores ranged between 0 and 1 and Q² scores between negative and 1, where a R²Y score of 1 demonstrated that the model explained 100% of variance, and a Q² score closer to 1 indicated higher reliability of the prediction in the cross-validation procedure. Validation of the OPLS-DA model was also performed by means of a permutation test (400 times). The R²Y in the permuted plot described

how well the data fitted with the derived model, whereas Q^2 described the predictive ability of the derived model ($Q^2 > 0.5$ considered as good and $Q^2 > 0.9$ as excellent). To further evaluate the predictive power of the robust OPLS-DA model, 80% of samples were applied to construct a model, which was used to predict the remaining 20% of samples. The variable importance in the projection (VIP) values of all peaks from OPLS-DA models was taken as a coefficient for peak selection. The VIP value was represented by a unitless number, where higher values suggested greater discriminatory power of the metabolite. Those variables with $VIP > 1$ were considered potential biomarker candidates for group discrimination.

Statistical analysis

The relative concentrations of those metabolites with $VIP > 1$ were calculated by integrating the signals in the spectra. Statistical significance was assessed using the Mann-Whitney U test, and $P < 0.05$ was considered statistically significant. The relative concentrations of those metabolites with $VIP > 1$ were calculated by integrating the signals in the spectra, and data are presented as the mean fold difference in EC metabolite abundance compared to controls. To further evaluate the diagnostic power of the potential biomarkers whose levels significantly differed between experimental groups, receiver operating characteristic (ROC) analysis in SPSS version 16.0 was performed, and the optimal area under the ROC curve (AUROC), specificity and sensitivity of the metabolites were calculated, where $AUROC > 0.8$ indicated excellent diagnostic ability. Pearson correlation analysis was used to assess the association of biomarker candidates between urine and tumor tissues of EC patients with an OPLS-DA model using a correlation coefficient cut-off of $|r|$ and correlation significance of $P < 0.05$. Correlation coefficients ranged from 1.0 (maximum positive correlation) to -1.0 (maximum anticorrelation), with a value of 0 representing no correlation. Correspondingly, $|r| > 0.44$ (calculated for the sample size of 20) was considered to be a statistically significant relationship between the two metabolites.

RESULTS

Metabolic profiles of esophageal tissues and urine samples

Representative 1D ^1H -NMR spectra of urine specimens acquired from EC patients, HCs and patient-matched esophageal tissue extracts are shown in **Figure 1A** and **B**. The standard 1D spectrum gave an overview of all metabolites. The major metabolites in the spectra were identified according to previous studies^[17,18] and the Human Metabolome Database (<http://www.hmdb.ca/>). In all urine and esophageal tissue spectra, the aliphatic region at 0.8–4.2 ppm included numerous signals from the following water-soluble metabolites: Glutamate, glutamine, acetoacetate, citrate, cisaconitate, choline, creatine, creatinine and glycine, which are known to be involved in many biochemical processes, especially in energy metabolism.

Good discrimination between EC patients and HCs was achieved by an OPLS-DA scores plot generated from ^1H -NMR spectra of urine specimens (**Figure 2A-a**). The predictive ability of the model was calculated by internal validation ($R^2Y = 0.902$, $Q^2 = 0.682$, CV-ANONA $P < 0.01$), suggesting that the model possessed a satisfactory fit with good predictive power. In order to evaluate the robustness of the OPLS-DA model described above, a random permutation test was performed 400 times to further evaluate the robustness of this model, as exhibited by the steep R^2 and Q^2 regression lines and difference between R^2 and Q^2 ($R^2Y = 0.886$ and $Q^2 = 0.660$), indicating that this was an excellent model suitable for data analysis (**Figure 2A-b**). To further assess the predictive ability of the model for unknown samples, we randomly selected 80% of urine samples ("training set", 33 EC patients and 32 HCs) to construct an OPLS-DA model, which was then used to predict the remaining 20% of samples ("testing set", 8 EC patients and 8 HCs). As can be seen in **Figure 2A-c**, the testing sets of EC patients and HCs were correctly located in their corresponding region of the training sets. Urine metabolites that met the following conditions were considered potential metabolite biomarkers for EC detection: Levels of metabolites with $VIP > 1$ and the presence of a significant difference ($P < 0.01$) between metabolite levels of EC patients and HCs according to the Mann-Whitney U test. A total of ten urine metabolites were found to be significantly changed in EC patients compared to HCs (**Table 2**), including higher levels of acetoacetate, cis-aconitate, citrate and glutamate, together with lower amounts of glycine, taurine, creatinine, ethanolamine, glucose and hippurate.

Tissue profiles from EC tumor tissues and their corresponding adjacent noncancerous tissues were clearly separated using the OPLS-DA scores plot (**Figure**

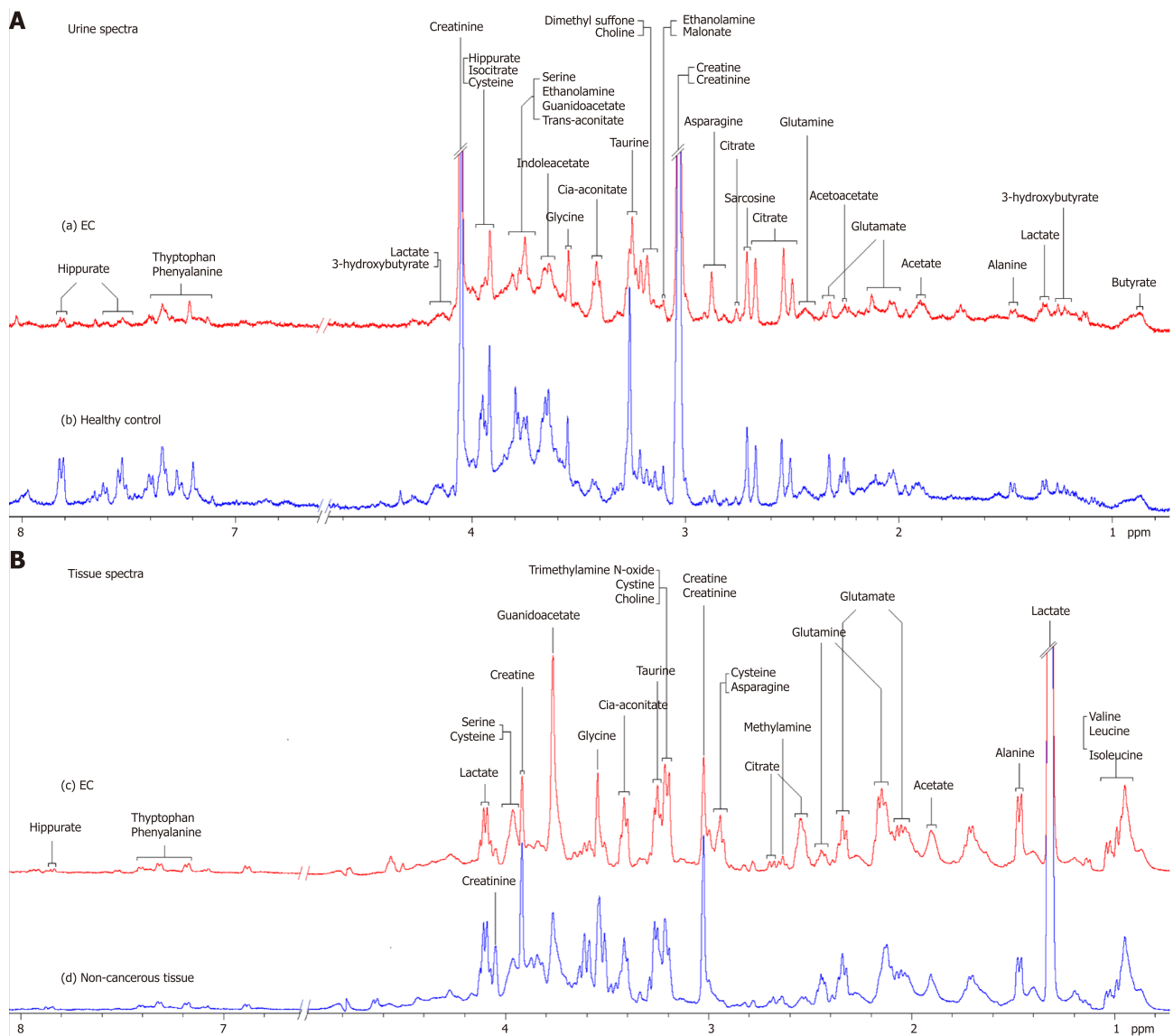


Figure 1 Proton nuclear magnetic resonance spectra. A: 400 MHz representative urine proton nuclear magnetic resonance (^1H -NMR) spectra obtained from esophageal cancer (EC) patient (a) and healthy control (b); B: Tissue ^1H -NMR spectra obtained from EC tissue (c) and adjacent noncancerous tissue (d) referenced to tetrauteriopropanate (0.0 ppm).

2B-a). Model parameters of the 400 times permutation test generated $R^2Y = 0.908$ and $Q^2 = 0.842$ (Figure 2B-b). Moreover, the OPLS-DA model showed good performance for predicting the unknown samples (Figure 2B-c). Using these criteria ($VIP > 1$ and $P < 0.05$), the 15 metabolites listed in Table 3 were found to be significantly changed in EC tissues compared to their corresponding noncancerous tissues, including elevated levels of valine, leucine, alanine, acetate, citrate, succinate, choline and glutamate, as well as depleted levels of creatinine and creatine, glycine, threonine, taurine, glucose, and glutamine.

Metabolic changes that overlap across urine and EC tissues

Our parallel investigations revealed a few distinct and overlapping discriminatory metabolites between cancer tissues and urine of EC patients, including decreased levels of glucose, glycine, creatinine and taurine, together with increased levels of glutamate and citrate, as compared to their respective controls. Metabolic profiling associations between potential urine and tissue biomarkers were further analyzed, plotted as correlation heat maps color-coded by the strength of Spearman correlation coefficients (Figure 3). Changes in most potential urinary biomarkers (except for glutamate, citrate and glucose) were found to be correlated with changes in most biomarker candidates in EC tissues (except for glycine and acetate) ($|r| > 0.44$, $P < 0.05$).

Comparison of diagnostic performance of potential urinary biomarkers for

Table 2 Potential urine biomarkers for discriminating esophageal cancer patients from healthy controls

Metabolite	Chemicalshift, ppm	Fold difference		AUC (95%CI)	Related metabolic pathways
		EC / HC	P value		
Acetoacetate	2.25–2.28	1.55 ↑	< 0.001	0.745 (0.636–0.836)	Fatty acid metabolism, TCA cycle
Glutamate	2.04–2.06	1.22 ↑	0.002	0.702 (0.590–0.798)	Glutaminolysis, TCA cycle
Cis-aconitate	3.40–3.46	1.30 ↑	0.001	0.719 (0.608–0.813)	TCA cycle, glyoxylate and dicarboxylate metabolism
Citrate	2.48–2.54 2.64–2.66	1.27 ↑	0.002	0.643 (0.528–0.746)	TCA cycle
Hippurate	7.51–7.56 7.60–7.65 7.78–7.84	0.45 ↓	0.002	0.702 (0.591–0.799)	Gut microflora metabolism
Ethanolamine	3.08–3.16	0.86 ↓	0.001	0.723 (0.613–0.817)	Fatty acid metabolism
Glycine	3.54–3.55	0.85 ↓	0.003	0.633 (0.518–0.737)	Amino acid metabolism
Creatinine	3.03–3.06 4.05–4.10	0.95 ↓	< 0.001	0.790 (0.685–0.872)	Urea metabolism, Creatinine metabolism
Taurine	3.26–3.28	0.53 ↓	< 0.001	0.763 (0.655–0.850)	Amino acid metabolism
Glucose	3.73–3.80	0.89 ↓	0.007	0.694 (0.581–0.792)	Glycolysis; TCA cycle

EC: Esophageal cancer; HC: Healthy control; AUC: Area under the curve; TCA: Tricarboxylic acid.

distinguishing EC

Given that urinary glutamate, citrate and glucose in EC patients did not show correlation with esophageal tissue biomarkers, a panel of urinary metabolite markers composed of acetoacetate, cis-aconitate, hippurate, ethanolamine, glycine, creatinine and taurine was selected to compare their diagnostic performance for distinguishing EC patients from HCs. ROC analysis of the comparison of single urinary biomarkers and their combination showed that combined metabolites of the aforementioned metabolites had better diagnostic performance than any single metabolite alone in discriminating EC patients from HCs, with sensitivity, specificity and area under the curve values of 92.68%, 92.50% and 0.971, respectively (Figure 4).

DISCUSSION

The current study performed parallel investigations of EC tissues and adjacent noncancerous mucosal tissues alongside patient-matched urine samples to investigate how changes of the urine metabolome were linked to the changes of EC tissues metabolic phenotypes. Our study showed significant metabolic alterations in both urine and tumor tissues of EC patients compared to their respective HCs. Correlative analysis of the altered metabolites across both matrices revealed a few distinct and overlapping discriminatory metabolites, such as glucose, glycine, creatinine and taurine (decreased levels) together with glutamate and citrate (increased amounts), suggesting that EC is associated with the following dysregulated metabolic pathway perturbations, including but not limited to fatty acid metabolism, glucose and glycolytic activity, tricarboxylic acid (TCA) cycle and glutaminolysis. Metabolic profiling correlations between esophageal tissues and urine showed that most potential urine biomarkers were correlated with most of the discriminating metabolites in EC tissues, indicating that changes in urine metabolic signature could reflect reprogramming of metabolic pathways in tumor tissues, highlighting the significance of the distinct urinary metabolic profiles as potential novel and noninvasive indicators for EC detection.

Our NMR-based metabolomic findings identified distinct disturbances occurring in both tissues and urine of EC patients compared to their respective controls (Figure 5). Tumor-microenvironment cooperation may occur in cancer cells, which exhibit a high rate of anabolic metabolism, by which they take up large amounts of nutrients to fuel the TCA cycle and oxidative phosphorylation. Therefore, in order to meet the increased demands of proliferation, tumor cells display changes in energy metabolism and nutrient uptake pathways^[19]. In general, tumor tissue has depleted glucose and increased citrate and succinate, the TCA intermediates, reflecting high TCA cycle activity to maintain tumor promotion^[8,20]. Reduced glucose and increased citrate levels were evident in EC patient urine, further indicating enhanced glycolysis under hypoxic conditions required for rapid cancer cell proliferation^[21,22]. Acetate, a source for lipid and myelin synthesis^[23], is derived from acetyl-CoA *via* the deacetylation of N-

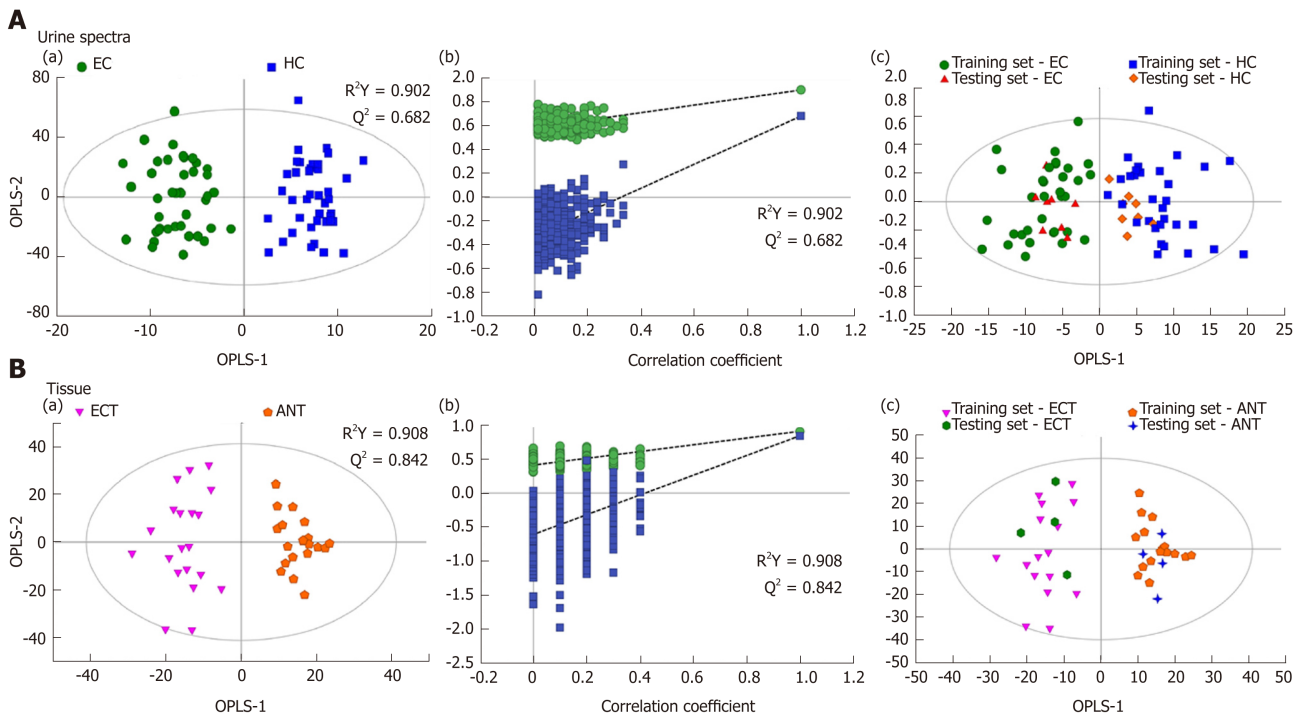


Figure 2 Pattern recognitions. A: Pattern recognition of urine metabolomic profiles analyzed by proton nuclear magnetic resonance (^1H -NMR) spectroscopy. (a) orthogonal partial least squares discriminant analysis (OPLS-DA) scatter plot of urine samples based on esophageal cancer (EC) patients (green dots) and healthy controls (HCs) (blue squares); (b) Statistical validation of the corresponding OPLS-DA model by permutation analysis (400 times); (c) Score plots of OPLS-DA prediction model. 80% of samples were applied to construct the model, which was used to predict the remaining 20% of samples [testing set, 8 HCs (gold diamonds); 8 EC patients (red triangles)]; B: Pattern recognition of tissue metabolomic profiles analyzed by ^1H -NMR spectroscopy. (a) OPLS-DA scatter plot of EC tissue samples obtained (purple inverted triangles) and adjacent noncancerous tissue (orange pentagons); (b) Statistical validation of the corresponding OPLS-DA model by permutation analysis (400 times); (c) Score plots of OPLS-DA prediction model, with 80% of the samples applied to construct the model, which was used to predict the remaining 20% of samples [testing set, 4 EC tissues (green hexagons); 4 adjacent non-cancerous tissues (blue crosses)].

acetylaspertate. The observed elevation of acetate in EC tissues might result from an increase in fatty acid metabolism, and this observation is supported by elevation of alanine derived from metabolism of pyruvate, indicating activation of glycolysis to provide higher energy needs^[24]. Glutamine is also regarded as important for energy production in proliferating cells, and it donates nitrogen for nucleotide synthesis, resulting in the formation of glutamate (glutaminolysis). The latter can be converted to α -ketoglutarate to increase transit through the TCA cycle, providing sustainable energy required for rapid cell proliferation^[25]. Therefore, increased glutamate along with depleted glutamine in EC tissue could suggest changes in glutaminolytic activity for EC development. The increased glutamate in EC urine observed in this study could also suggest a high energy demand in proliferating cells due to augmented glutaminolysis^[26]. Increased leucine and valine in tissues and increased acetoacetate in urine were in agreement with the ingested nutrients that fuel the TCA cycle to support cell proliferation. Similarly, cell growth and proliferation need amino acids to generate proteins required for cancer cell synthesis^[27], therefore leading to decreased levels of glycine and threonine in EC patients. Depleted creatine/creatinine levels in tumor tissues have been related to altered energy transfer processes and may reflect increased activity of creatine kinase, which has been previously reported to be lower in lung tumors compared to normal adjacent tissues^[28]. Besides, creatinine levels in EC patient urine samples were significantly decreased compared to HCs, which has also been reported to be lower in urine samples from colorectal cancer patients^[7]. The observed depletion of taurine in both tissues and urine of EC patients suggest a disruption in taurine metabolism and diffusion of gut microbes associated with EC tumors^[29]. Ethanolamine is an important fatty acid for cellular membranes^[30], and its decreased levels in EC urine could suggest increased consumption for biosynthesis of cellular membranes and indicate activation of fatty acid metabolism. The observed depletion of hippurate in EC urine was likely the result of gut microbiome perturbation associated with EC tumorigenesis. Hippurate is metabolized from benzoic acid, which is metabolized from the dietary polyphenol 3-hydroxyphenyl propionic acid by the gut microflora^[31]. Choline is one of the major cell membrane phospholipids^[32] and is overexpressed and highly active in tumor tissues and cell lines. We observed increased choline levels in EC tissues, which was consistent with previous

Table 3 Potential tissue biomarkers for discriminating esophageal cancer tissue from adjacent noncancerous tissue

Metabolite	Chemicalshift, ppm	Fold difference		AUC (95%CI)	Related metabolic pathways
		ECT / ANT	P value		
Valine	0.96–0.99 1.02–1.04	1.63 ↑	< 0.001	0.988 (0.889–1.000)	Amino acid metabolism
Leucine	0.93–0.95	1.32 ↑	< 0.001	0.852 (0.705–0.944)	Amino acid metabolism
Glutamate	1.97–2.08 2.32–2.39	1.30 ↑	< 0.001	0.930 (0.803–0.986)	Glutaminolysis, TCA cycle
Acetate	1.88–1.93	1.33 ↑	0.001	0.790 (0.632–0.902)	SCFA metabolism
Alanine	1.43–1.48	1.44 ↑	< 0.001	0.920 (0.789–0.982)	Amino acid metabolism, Gluconeogenesis
Choline	3.19–3.22	1.59 ↑	< 0.001	0.980 (0.876–1.000)	Choline metabolism, Lipid metabolism
Succinate	2.39–2.40	2.12 ↑	0.009	0.738 (0.575–0.864)	TCA cycle
Citrate	2.68–2.71	1.42 ↑	< 0.001	0.942 (0.820–0.991)	TCA cycle
Glucose	3.37–3.44 3.50–3.52	0.72 ↓	< 0.001	0.928 (0.800–0.985)	Glycolysis, TCA cycle
Creatinine	3.02–3.03 4.04–4.06	0.64 ↓	< 0.001	0.963 (0.849–0.997)	Urea metabolism, Creatine metabolism
Glycine	3.52–3.55	0.75 ↓	< 0.001	0.850 (0.702–0.943)	Amino acid metabolism
Threonine	3.58–3.62	0.60 ↓	< 0.001	0.933 (0.806–0.987)	Amino acid metabolism
Creatine	3.90–3.94	0.78 ↓	< 0.001	0.917 (0.786–0.981)	Urea metabolism, Creatine metabolism
Glutamine	2.42–2.48	0.77 ↓	< 0.001	0.895 (0.757–0.969)	Glutaminolysis, TCA cycle
Taurine	3.24–3.28 3.33–3.34	0.78 ↓	< 0.001	0.878 (0.735–0.960)	Amino acid metabolism

ANT: Adjacent noncancerous tissue; ECT: Esophageal cancer tissue; AUC: Area under the curve; TCA: Tricarboxylic acid.

reports^[7], indicating that choline could be a viable tissue biomarker as-associated with tumor promotion. However, this biomarker of EC tumor tissue was not completely detectable at the end of metabolism of urine biomarkers in this study.

In addition to specific metabolite differences between tumor tissues and urine in EC patients and HCs, we also evaluated the relationships between the metabolic networks in both tissues and urine. Decreased metabolite levels of glucose, glycine, creatinine and taurine, as well as increased citrate and glutamate in EC tissues, were also detectable in the urine of EC patients. These distinct and overlapping metabolites may reflect tumor cell shedding and represent metabolic pathway aberrations across both matrices. This potentially reveals linkages to disturbances of fatty acid metabolism, glucose and glycolytic activity, TCA cycle and glutaminolysis associated with tumor proliferation. Correlative analysis of metabolic profiling between EC tissues and urine showed that changes in most potential urinary biomarkers were correlated with changes in most biomarker candidates in EC tissues, implying enhanced energy production required for rapid cell proliferation. Creatinine was found to be the most sensitive predictor of EC in urine metabolite, with an AUC of 0.790. Overall, these associations provide evidence of distinct metabolic signatures and pathway disturbances across both matrices, and changes in urinary metabolic signature could reflect the EC tissue microenvironment.

In conclusion, our parallel investigations of EC patients through ¹H-NMR metabolomics revealed a great number of altered metabolites and metabolic pathway networks in EC patient urine and tumor tissues compared with HCs. We identified a few overlapping discriminatory metabolites across both matrices, derived from fatty acid metabolism (taurine and glycine), as well as metabolites (*e.g.*, glucose, glutamate, citrate and creatinine) involved in glucose and glycolytic metabolism, the TCA cycle and glutaminolysis. Correlative analysis of metabolic profiling across tumor tissues and urine in EC patients showed that changes in most potential urinary biomarkers were correlated with changes in most candidate biomarkers in EC tissues, implying enhanced energy production required for rapid cell proliferation. In summary, these associations provide clear evidence of different metabolic signatures and metabolic pathway disturbances between EC tissues and urine, and changes in urinary metabolic signatures could reflect the EC tissue microenvironment. Our study highlighted the significance of the distinct urinary metabolic profile as a potential noninvasive indicator of EC detection. Further investigation is needed to validate these initial findings using larger samples and to establish the mechanism underlying EC progression.

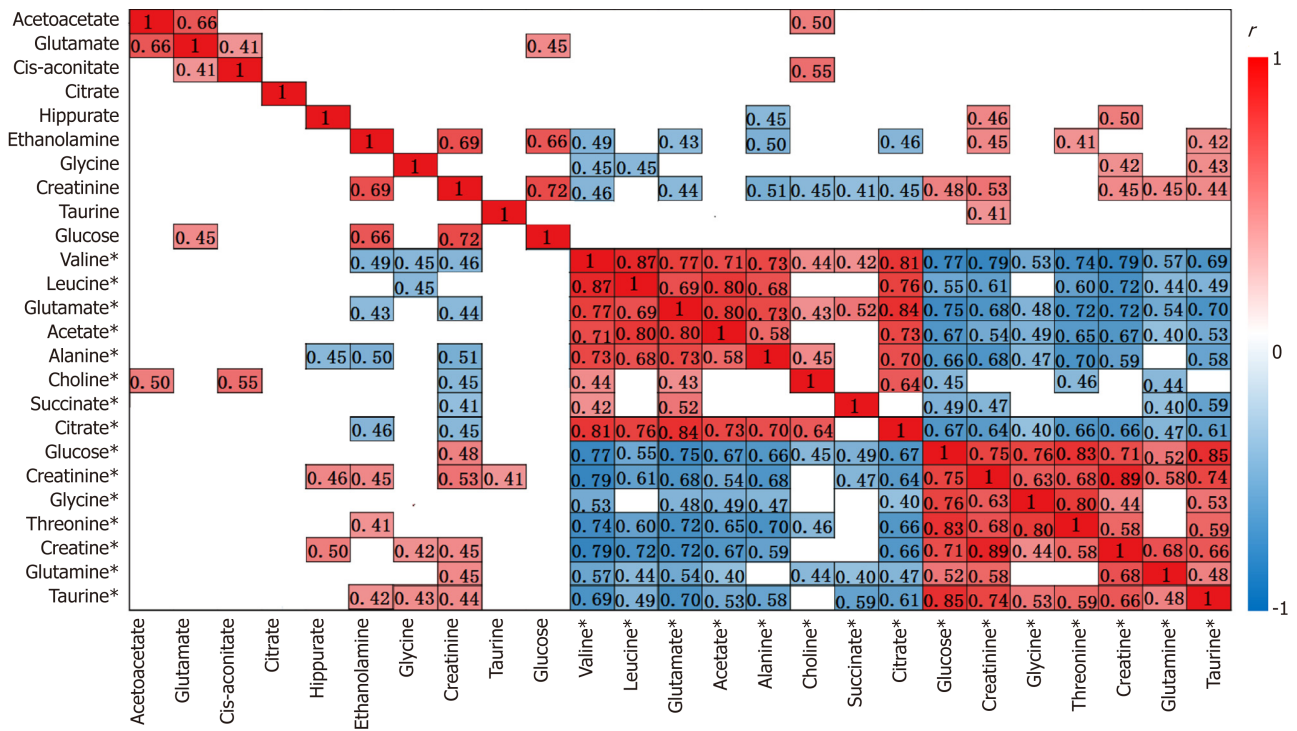


Figure 3 Correlation heat map color-coded by the strength of Spearman correlation coefficients (r) between metabolites found to be important in tumor versus control discrimination. Cut-off values of $|r| > 0.4$ and $P < 0.05$ have been used. The metabolites used are those listed in Tables 2 and 3 (metabolites labeled with "*" noted as tissue biomarkers). Red boxes indicate positive associations, and blue boxes indicate negative associations.

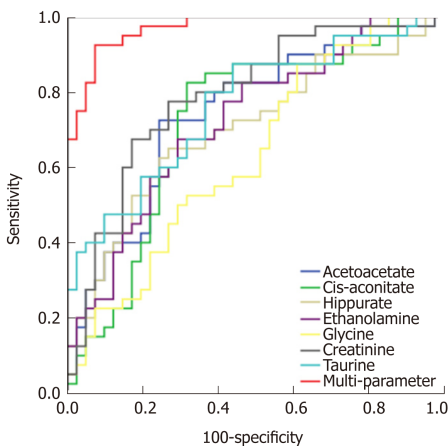


Figure 4 Comparison of single and combined metabolites receiver operating characteristic curves for distinguishing esophageal cancer patients from healthy controls.

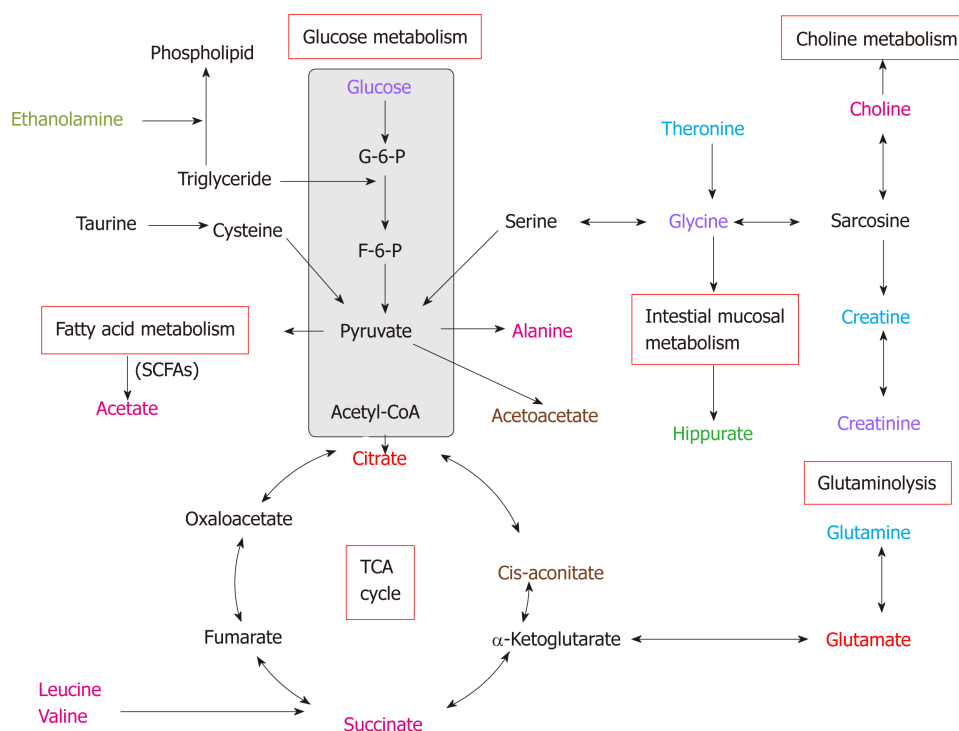


Figure 5 Altered metabolic pathways for the most relevant distinguishing metabolites (potential biomarkers) in urine and tissue samples between esophageal cancer patients and healthy controls. Red text: Increased with respect to control in both esophageal cancer (EC) patient tissue and urine; pink text: Increased with respect to control in EC tissue; orange text: Increased with respect to control in EC patient urine; purple text: Decreased with respect to control in both EC patient tissue and urine; blue text: Decreased with respect to control in EC tissue; green text: Decreased with respect to control in EC patient urine.

ARTICLE HIGHLIGHTS

Research background

A large number of studies have revealed changes of urinary metabolites between esophageal cancer (EC) and healthy controls (HCs), and some studies have demonstrated a correlation between EC and perturbed urinary metabolomic profiles.

Research motivation

However, none of the previous studies has described the correlation between urine metabolite profiles and those of the tumor and adjacent colonic mucosa in the same patient. Our study revealed a significant number of altered metabolites and metabolic pathway networks in EC patient urine and tumor tissues compared with HCs.

Research objectives

Our work is the first parallel investigation of esophageal tumor tissues and adjacent normal mucosal tissues alongside patient-matched urine samples to investigate how urinary metabolic phenotypes were linked to changes in the biochemical landscape of esophageal tumors.

Research methods

All samples were detected by a Bruker AVII 400 MHz nuclear magnetic resonance spectrometer, and all spectral data were applied to pattern recognition analysis and cross-validation by SIMCA-P software. Then, statistical significance was assessed using the Mann-Whitney *U* test and receiver operating characteristic analysis to calculate biomarker metabolites. Finally, we employed Pearson Correlation Analysis to assess the associations of biomarker candidates between urine and tumor tissues of EC patients.

Research results

Our study revealed metabolite changes that overlapped across both metrics, including glucose, glutamate, citrate, glycine, creatinine and taurine, indicating the networks for metabolic pathway perturbations in EC. Additionally, changes in most urinary biomarkers were correlated with changes in biomarker candidates in EC tissues.

Research conclusions

Our research is the first parallel investigation to investigate how urinary metabolic phenotypes were linked to the changes in the biochemical landscape of esophageal tumors. Our study showed significant metabolic alterations in both urine and tumor tissues of EC patients compared to their respective HCs. Our research revealed a few distinct and overlapping discri-

minatory metabolites, suggesting that EC is associated with the following dysregulated metabolic pathway perturbations. Furthermore, the metabolic profiling correlations between esophageal tissues and urine showed that most urine potential biomarkers were correlated with most of the discriminating metabolites in EC tissues, indicating that changes in the urine metabolic signature could reflect reprogramming of metabolic pathways in tumor tissue, highlighting the significance of the distinct urinary metabolic profiles as potential novel and non-invasive indicators for EC detection.

Research perspectives

With experiences in our study, we realized that many metabolites have associations in samples of cancer patients. In our same group, we are now investigating the serum samples of EC patients to see whether the same pattern of serum levels of amino acids can be found in EC patients.

ACKNOWLEDGEMENTS

The authors thank Ju-Rong Yang for kindly providing us with the NMR experimental setting and Dr. Hong-Jun Luo for handling of tissue samples.

REFERENCES

- 1 Ferlay J, Soerjomataram I, Dikshit R, Eser S, Mathers C, Rebelo M, Parkin DM, Forman D, Bray F. Cancer incidence and mortality worldwide: sources, methods and major patterns in GLOBOCAN 2012. *Int J Cancer* 2015; **136**: E359-E386 [PMID: 25220842 DOI: 10.1002/ijc.29210]
- 2 Lindon JC, Nicholson JK, Holmes E, Everett JR. Metabonomics: metabolic processes studied by NMR spectroscopy of biofluids. *Magnetic Resonance An Ed J* 2015; **12**: 289-320 [DOI: 10.1002/1099-0534(2000)12:5<289::AID-CMR3>3.0.CO;2-W]
- 3 Griffin JL, Atherton H, Shockcor J, Atzori L. Metabolomics as a tool for cardiac research. *Nat Rev Cardiol* 2011; **8**: 630-643 [PMID: 21931361 DOI: 10.1038/nrcardio.2011.138]
- 4 Lin Y, Stephenson MC, Xin L, Napolitano A, Morris PG. Investigating the metabolic changes due to visual stimulation using functional proton magnetic resonance spectroscopy at 7 T. *J Cereb Blood Flow Metab* 2012; **32**: 1484-1495 [PMID: 22434070 DOI: 10.1038/jcbfm.2012.33]
- 5 Duarte IF, Gil AM. Metabolic signatures of cancer unveiled by NMR spectroscopy of human biofluids. *Prog Nucl Magn Reson Spectrosc* 2012; **62**: 51-74 [PMID: 22364616 DOI: 10.1016/j.pnmrs.2011.11.002]
- 6 Lin Y, Ma C, Liu C, Wang Z, Yang J, Liu X, Shen Z, Wu R. NMR-based fecal metabolomics fingerprinting as predictors of earlier diagnosis in patients with colorectal cancer. *Oncotarget* 2016; **7**: 29454-29464 [PMID: 27107423 DOI: 10.18632/oncotarget.8762]
- 7 Wang Z, Lin Y, Liang J, Huang Y, Ma C, Liu X, Yang J. NMR-based metabolomic techniques identify potential urinary biomarkers for early colorectal cancer detection. *Oncotarget* 2017; **8**: 105819-105831 [PMID: 29285295 DOI: 10.18632/oncotarget.22402]
- 8 Lin Y, Ma C, Bezabeh T, Wang Z, Liang J, Huang Y, Zhao J, Liu X, Ye W, Tang W, Ouyang T, Wu R. 1 H NMR-based metabolomics reveal overlapping discriminatory metabolites and metabolic pathway disturbances between colorectal tumor tissues and fecal samples. *Int J Cancer* 2019 [PMID: 30720869 DOI: 10.1002/ijc.32190]
- 9 Nicholson JK, Lindon JC. Systems biology: Metabonomics. *Nature* 2008; **455**: 1054-1056 [PMID: 18948945 DOI: 10.1038/4551054a]
- 10 Rocha CM, Carrola J, Barros AS, Gil AM, Goodfellow BJ, Carreira IM, Bernardo J, Gomes A, Sousa V, Carvalho L, Duarte IF. Metabolic signatures of lung cancer in biofluids: NMR-based metabonomics of blood plasma. *J Proteome Res* 2011; **10**: 4314-4324 [PMID: 21744875 DOI: 10.1021/pr200550p]
- 11 Theodorescu D, Wittke S, Ross MM, Walden M, Conaway M, Just I, Mischak H, Frierson HF. Discovery and validation of new protein biomarkers for urothelial cancer: a prospective analysis. *Lancet Oncol* 2006; **7**: 230-240 [PMID: 16510332 DOI: 10.1016/S1470-2045(06)70584-8]
- 12 M'Koma AE, Blum DL, Norris JL, Koyama T, Billheimer D, Motley S, Ghiassi M, Ferdowsi N, Bhowmick I, Chang SS, Fowke JH, Caprioli RM, Bhowmick NA. Detection of pre-neoplastic and neoplastic prostate disease by MALDI profiling of urine. *Biochem Biophys Res Commun* 2007; **353**: 829-834 [PMID: 17194448 DOI: 10.1016/j.bbrc.2006.12.111]
- 13 Theodorescu D, Schiffer E, Bauer HW, Douwes F, Eichhorn F, Polley R, Schmidt T, Schöfer W, Zürgb P, Good DM, Coon JJ, Mischak H. Discovery and validation of urinary biomarkers for prostate cancer. *Proteomics Clin Appl* 2008; **2**: 556-570 [PMID: 19759844 DOI: 10.1002/prca.200780082]
- 14 Pisitkun T, Johnstone R, Knepper MA. Discovery of urinary biomarkers. *Mol Cell Proteomics* 2006; **5**: 1760-1771 [PMID: 16837576 DOI: 10.1074/mcp.R600004-MCP200]
- 15 Hasim A, Ma H, Mamtimin B, Abudula A, Niyaz M, Zhang LW, Anwer J, Sheyhidin I. Revealing the metabonomic variation of EC using ¹H-NMR spectroscopy and its association with the clinicopathological characteristics. *Mol Biol Rep* 2012; **39**: 8955-8964 [PMID: 22736106 DOI: 10.1007/s11033-012-1764-z]
- 16 Davis VW, Schiller DE, Eurich D, Sawyer MB. Urinary metabolomic signature of esophageal cancer and Barrett's esophagus. *World J Surg Oncol* 2012; **10**: 271 [PMID: 23241138 DOI: 10.1186/1477-7819-10-271]
- 17 Wishart DS, Jewison T, Guo AC, Wilson M, Knox C, Liu Y, Djoumbou Y, Mandal R, Aziat F, Dong E, Bouatra S, Sinelnikov I, Arndt D, Xia J, Liu P, Yallou F, Bjorn Dahl T, Perez-Pineiro R, Eisner R, Allen F, Neveu V, Greiner R, Scalbert A. HMDB 3.0--The Human Metabolome Database in 2013. *Nucleic Acids Res* 2013; **41**: D801-D807 [PMID: 23161693 DOI: 10.1093/nar/gks1065]
- 18 Bouatra S, Aziat F, Mandal R, Guo AC, Wilson MR, Knox C, Bjorn Dahl TC, Krishnamurthy R, Saleem F, Liu P, Dame ZT, Poelzer J, Huynh J, Yallou FS, Psychogios N, Dong E, Bogumil R, Roehring C, Wishart DS. The human urine metabolome. *PLoS One* 2013; **8**: e73076 [PMID: 24023812 DOI: 10.1371/journal.pone.0073076]

- 19 **Jones RG**, Thompson CB. Tumor suppressors and cell metabolism: a recipe for cancer growth. *Genes Dev* 2009; **23**: 537-548 [PMID: [19270154](#) DOI: [10.1101/gad.1756509](#)]
- 20 **Selak MA**, Armour SM, MacKenzie ED, Boulahbel H, Watson DG, Mansfield KD, Pan Y, Simon MC, Thompson CB, Gottlieb E. Succinate links TCA cycle dysfunction to oncogenesis by inhibiting HIF- α prolyl hydroxylase. *Cancer Cell* 2005; **7**: 77-85 [PMID: [15652751](#) DOI: [10.1016/j.ccr.2004.11.022](#)]
- 21 **Vander Heiden MG**, Cantley LC, Thompson CB. Understanding the Warburg effect: the metabolic requirements of cell proliferation. *Science* 2009; **324**: 1029-1033 [PMID: [19460998](#) DOI: [10.1126/science.1160809](#)]
- 22 **Echeverry G**, Hortin GL, Rai AJ. Introduction to urinalysis: historical perspectives and clinical application. *Methods Mol Biol* 2010; **641**: 1-12 [PMID: [20407938](#) DOI: [10.1007/978-1-60761-711-2_1](#)]
- 23 **Phelps TJ**, Suflita JM, Little B. Carbon dioxide corrosion and acetate: a hypothesis on the influence of microorganisms. *Corrosion Houston Tx* 2012; **64**: 854-859 [DOI: [10.5006/1.3279919](#)]
- 24 **Chen JQ**, Russo J. Dysregulation of glucose transport, glycolysis, TCA cycle and glutaminolysis by oncogenes and tumor suppressors in cancer cells. *Biochim Biophys Acta* 2012; **1826**: 370-384 [PMID: [22750268](#) DOI: [10.1016/j.bbcan.2012.06.004](#)]
- 25 **Curthoys NP**, Watford M. Regulation of glutaminase activity and glutamine metabolism. *Annu Rev Nutr* 1995; **15**: 133-159 [PMID: [8527215](#) DOI: [10.1146/annurev.nu.15.070195.001025](#)]
- 26 **Cairns RA**, Harris IS, Mak TW. Regulation of cancer cell metabolism. *Nature Reviews Cancer* 2011; **11**: 85
- 27 **Locasale JW**. Serine, glycine and one-carbon units: cancer metabolism in full circle. *Nat Rev Cancer* 2013; **13**: 572-583 [PMID: [23822983](#) DOI: [10.1038/nrc3557](#)]
- 28 **Joseph J**, Cardesa A, Carreras J. Creatine kinase activity and isoenzymes in lung, colon and liver carcinomas. *Br J Cancer* 1997; **76**: 600-605 [PMID: [9303358](#)]
- 29 **van Stijn MF**, Vermeulen MA, Siroen MP, Wong LN, van den Tol MP, Ligthart-Melis GC, Houdijk AP, van Leeuwen PA. Human taurine metabolism: fluxes and fractional extraction rates of the gut, liver, and kidneys. *Metabolism* 2012; **61**: 1036-1040 [PMID: [22304837](#) DOI: [10.1016/j.metabol.2011.12.005](#)]
- 30 **Amelio I**, Cutruzzolà F, Antonov A, Agostini M, Melino G. Serine and glycine metabolism in cancer. *Trends Biochem Sci* 2014; **39**: 191-198 [PMID: [24657017](#) DOI: [10.1016/j.tibs.2014.02.004](#)]
- 31 **Nicholson JK**, Holmes E, Wilson ID. Gut microorganisms, mammalian metabolism and personalized health care. *Nat Rev Microbiol* 2005; **3**: 431-438 [PMID: [15821725](#) DOI: [10.1038/nrmicro1152](#)]
- 32 **Pun WK**, Chow SP, Fang D, Cheng CL, Leong JC, Ng C. Post-traumatic oedema of the foot after tibial fracture. *Injury* 1989; **20**: 232-235 [PMID: [2592102](#) DOI: [10.1586/14737159.2015.1039515](#)]



Published By Baishideng Publishing Group Inc
7041 Koll Center Parkway, Suite 160, Pleasanton, CA 94566, USA
Telephone: +1-925-2238242
Fax: +1-925-2238243
E-mail: bpgoffice@wjgnet.com
Help Desk: <http://www.f6publishing.com/helpdesk>
<http://www.wjgnet.com>

